

Research Paper**THE GEOLOGY OF MOUNT ORLIAKAS AND THE PINDOS OPHIOLITE, GREECE****Kevin Wong^{1,2,*}, Kathryn Draper², Linshu Feng², Philip Hawkins², Samuel Oakley², Xiao Xu Zheng²**¹School of Earth and Environment, University of Leeds, Leeds, UK, LS2 9JTeekw@leeds.ac.uk²Department of Earth Sciences, University of Cambridge, Cambridge, CB2 3EQk_draper@live.co.uk lf373@cam.ac.uk, philhawkins@me.comsammy.oakley@btinternet.com, xiao_xu@live.nl**Correspondence to:**Kevin Wong
eekw@leeds.ac.uk**DOI number:**<http://dx.doi.org/10.12681/bgsg.19376>**Keywords:**

geological map, Pindos Ophiolite; Mesohellenic Trough; Mount Orliakas, Pindos Mountains

Citation:

Wong, K., Draper, K., Feng, L., Hawkins, P., Oakley, S. and Zheng, X. (2019), The Geology of Mount Orliakas and the Pindos Ophiolite, Greece. Bulletin Geological Society of Greece, 54, 144-177.

Publication History:Received: 17/12/2018
Accepted: 18/10/2019
Accepted article online: 27/12/2019

The Editor wishes to thank two anonymous reviewers for their work with the scientific reviewing of the manuscript and Dr. Petros Koutsovitis and Ms Emmanouela Konstantakopoulou for editorial assistance.

©2019. The Authors

This is an open access article under the terms of the Creative Commons Attribution License, which permits use, distribution and reproduction in any medium, provided the original work is properly cited.

Abstract

The Greveniotiki Pindos Mountains of Greece showcases the tectonics affecting the Central Mediterranean; however, no detailed geological maps have been produced of the region. In this study we present a 1:10,000 geological map of Mount Orliakas and its surrounding areas, including the westernmost parts of the Pindos Ophiolite complex and the Mesohellenic basin. With this map we provide accompanying lithological and structural discussions of the geology of the mapped region.

Keywords: geological map, Pindos Ophiolite, Mesohellenic Trough, Mount Orliakas, Pindos Mountains

Περίληψη

Η Γρεβενιώτικη οροσειρά της Πίνδου προβάλλει την τεκτονική που επηρεάζει την Κεντρική Μεσόγειο, ωστόσο, δεν έχουν εκπονηθεί λεπτομερείς γεωλογικοί χάρτες στην συγκεκριμένη περιοχή. Σε αυτή τη μελέτη παρουσιάζουμε ένα γεωλογικό χάρτη 1:10.000 του Όρους Ορλιακάς και των γύρω περιοχών, συμπεριλαμβανομένων των δυτικότερων τμημάτων του οφιολιθικού συμπλέγματος της Πίνδου και της Μεσοελληνικής αύλακας. Με τον χάρτη αυτό παρέχουμε συνοδευτικές λιθολογικές και γεωτεκτονικές πληροφορίες και στοιχεία για τη γεωλογία της εν λόγω περιοχής.

Λέξεις κλειδιά: γεωλογικός χάρτης, Οφιόλιθοι Πίνδου, Μεσοελληνική αύλακα, οροσειρά Όρλιακα; οροσειρά Πίνδου

1. INTRODUCTION

Mount Orliakas, of the Pindos Mountains of Northern Greece, is a region where the tectonics affecting Greece during the early Cenozoic can be studied. Mount Orliakas is a 6 km long scarp of recrystallised rudist bivalve reefstone, stratigraphically emplaced above the Pindos Ophiolite, and positioned along the western margin of the Mesohellenic trough (e.g. Rassios, 2011). To its west lies the Pindos Ophiolite complex, a series of igneous lithologies thought to represent obducted oceanic lithosphere (e.g. Smith and Rassios, 2003).

Previous mapping of the region was performed by Brunn (1956), and the tectonostratigraphy of the region described in detail by Jones and Robertson (1991). Literature on the region has focused primarily on the emplacement of the Pindos Ophiolite (Smith, 1993; Rassios and Smith, 2000; Smith and Rassios, 2003; Rassios and Moores, 2006), and the formation and sedimentation of the Mesohellenic Trough (MHT; Zelilidis et al., 2002; Vamvaka et al., 2006); however the area around the Pindos Ophiolite and the neighbouring Mesohellenic Trough is geologically mapped at a poor resolution (no more than 1:50,000), which ultimately limits the resolution of tectonic development models, which are dependent on the understanding of local structural geology.

The aim of this study is therefore to produce a new geological map for Mount Orliakas and the areas immediately around it. This work is a collaboration of the undergraduate mapping projects produced by the authors at the University of Cambridge, and complements the 1:10,000 scale geological map of Mount Orliakas and the Pindos Ophiolite that is attached to this report.

1.1. Regional Setting

The Pindos Zone of Greece is the easternmost unit of the External Hellenides, tectonic zones of Greece that are considered to have formed on the Apulian subcontinent (Rassios, 2011; Fig. 1). The Pindos Zone formed from flysch deposits of the flanks of Apulia during the closure of the Tethys Ocean, with a likely provenance from the eastern Pelagonian subcontinent (Ananiadis et al., 2004).

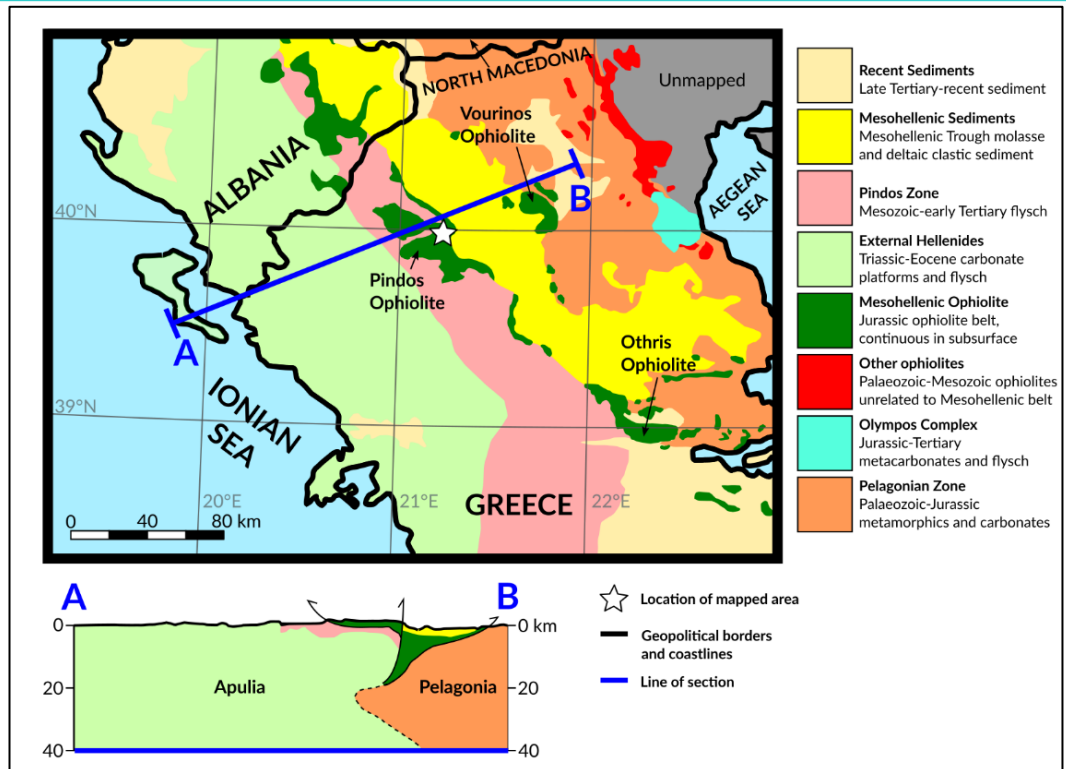


Fig. 1: Simplified geological map illustrating the major tectonic subdivision of northern Greece, redrawn after Rassios and Dilek (2009). The location of our mapped area is presented as a white star.

Formation of the Western Hellenic Ophiolites of Greece have been constrained through radiometric dating; K-Ar dating of ophiolitic sole hornblendes provide an ophiolite formation age of 172 ± 5 Ma (Thuizat et al., 1981), during which both oceanic seafloor spreading and intra-crustal thinning processes were likely active (Liati et al., 2004). Overthrusting of the Pindos Zone by the Western Hellenic Ophiolites occurred during the Eocene, emplacing the Pindos and West Othris ophiolites upon Pindos Zone flysch, and the East Othris and Vourinos ophiolites on basement rock (Papanikolaou, 2009; Rassios, 2011). Aeromagnetic mapping of the region suggests that the two sub-parallel ophiolite belts are continuous beneath the MHT, forming a single body often termed the Mesohellenic Ophiolite (Memou and Skianis, 1991). Kinematics within the ophiolite indicate a general north-east constrictive deformation resulting from emplacement from the south-west (Rassios and Moores, 2006). The formation of the MHT began shortly after the emplacement of the ophiolites, likely in response to the oblique convergence of the Apulian and Pelagonian subcontinents (Vamvaka et al., 2006). Sedimentation of the MHT began from the Eocene onward. As there are no post-Mesohellenic sediments in our region, formation of the Pindos mountain range likely coincided with the waning of sedimentation.

1.2. Regional geography

A 23 km² region of the Greveniotiki Pindos around Mount Orliakas was mapped, with its greatest extents at 21.2225°E - 39.9902°N and 21.3080°E - 40.0496°N, including the villages of Ziakas, Spelio, and Perivolaki. This region is bound the Venetikos River to the north, east, and south-east, and by roads to the west and the south-west. The terrain within the mapped area is extreme, limiting the degree of safely accessible outcrop. The most prominent topographic feature is the north-west to south-east-trending limestone ridge of Mount Orliakas, reaching a maximum of 1481m above sea level. The lowest topography encountered in the mapped region is the river valley of the Venetikos, which itself is most easily crossed at a stone bridge at Portitsa Gorge, a major geological feature in the region where the Venetikos River cuts through Mount Orliakas. Slopes between these extremes are very steep, especially in areas to the north of Orliakas, and around Portitsa Gorge. The best exposure is found along the roads bordering Mount Orliakas. A large portion of the region is covered in dense pine forest (especially in the ophiolitic section), limiting exposure significantly. Some bedrock is exposed along logging paths through the forest up towards the mountain. Gullies leading down to the Venetikos River also yield good bedrock exposure, albeit at the cost of high topographic gradients. Weather is variable in the Pindos. From mid-August to early September, cloud cover is low, and temperatures are high, with daily averages of 25°C. By mid-late September, thunderstorms are frequent and would often last for several days; during this time temperature fell to average 18°C. 1:5,000 field maps from the Hellenic Military Geographical Service (HMGS) were provided by Dr. Anne Rassios of the Institute of Geological and Mineralogical Exploration. Our final map (Supplementary Map) uses a modified version of the original HMGS grid, which we use to reference specific localities in this paper in addition to degrees latitude north and longitude east.

2. LITHOLOGICAL DESCRIPTIONS

The lithologies described within the mapped area broadly follow the nomenclature of Jones and Robertson (1991). Subdivisions and groupings of these units are assigned names based on their lithology and association at the discretion of the authors (Fig. 2). It is difficult to gauge stratigraphic thickness in the region as a result of extensive deformation; we have therefore produced a tectonostratigraphic column to aid in our description of stratigraphic relations within the mapped area.

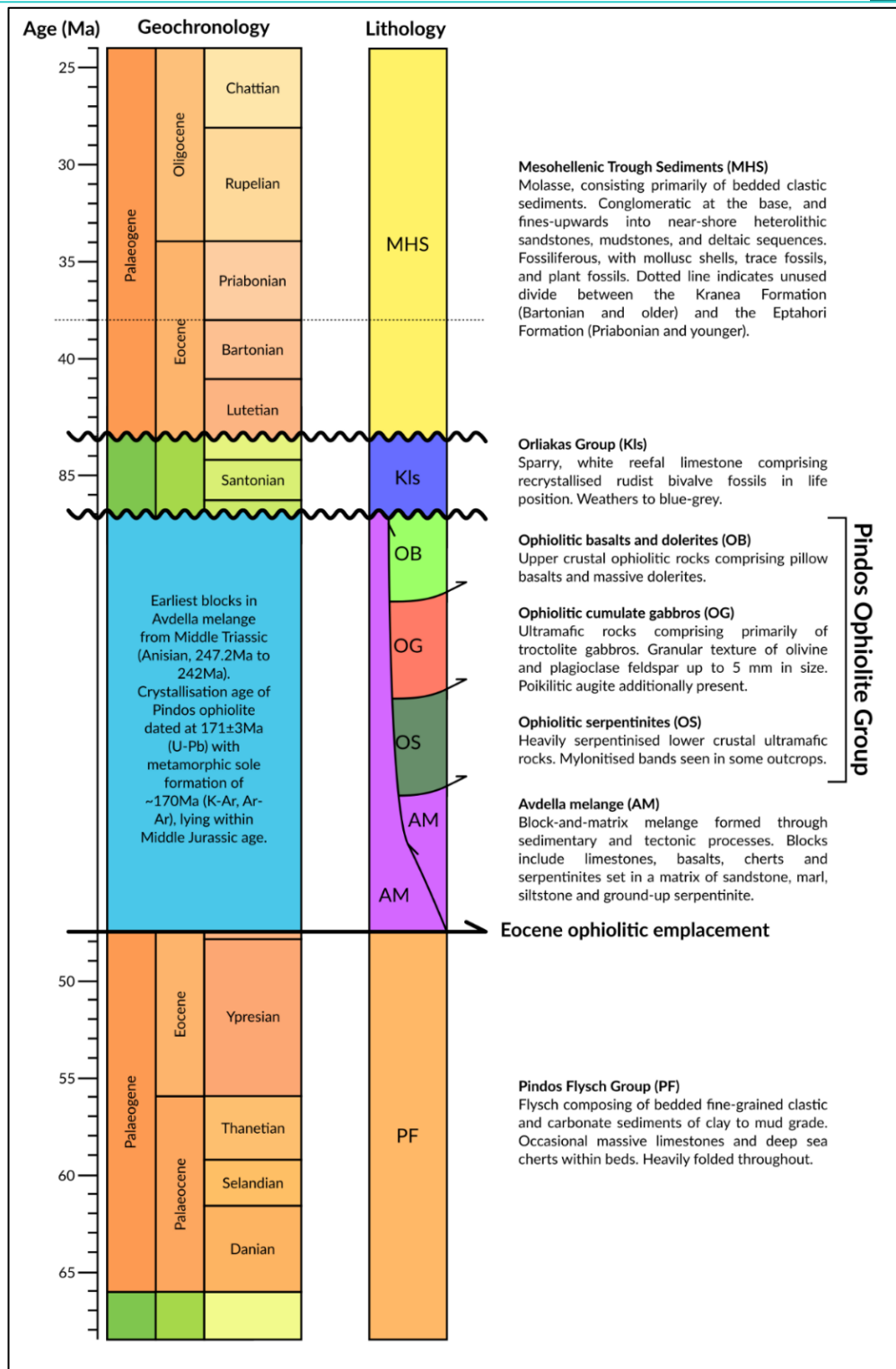


Fig. 2: Tectono-stratigraphic column of lithologies within the mapped area. Naming of mapped units is assigned after the nomenclature of Jones and Robertson (1991).

2.1. Sedimentary rocks

2.1.1. Pindos Flysch Group

The Pindos Flysch Group is a unit known throughout the Pindos Zone, bearing a regionally diachronous base (Faupl et al., 2007). This flysch is derived from both the Pindos Ophiolite to the west and the Pelagonian Zone to the east (Ananiadis et al., 2004). In the mapped region, the Pindos Flysch comprises grey-brown marls and clastic sediments ranging from clay to fine-sand grade, forming turbidite beds of 10-150 cm thickness. North of Orliakas, the flysch coarsens from east to west towards Perivolaki village, reaching a medium-grade sandstone at the village outskirts (-19990, -23915; 40.03526°N, 21.23417°E).

The petrological constituents forming flysch beds varies within outcrop-scale. Massive micritic limestone is observed within the flysch at (-20630, -25105; 40.02435°N, 21.22670°E), bearing small lens-shaped pockets of silt. Other parts of the flysch bear significant quantities of chert (e.g. -20135, -24710; 40.02794°N, 21.23272°E). Flysch clasts are difficult to petrologically identify in the field as a result of their very fine grain size; the abundance/absence of calcite crystals developing in cavities and forming veins within the flysch matrix are broadly indicative of the carbonate content present within the flysch as a whole. All the flysch is folded (Fig. 3), with fold wavelengths ranging from 10s of centimetres to hundreds of metres.

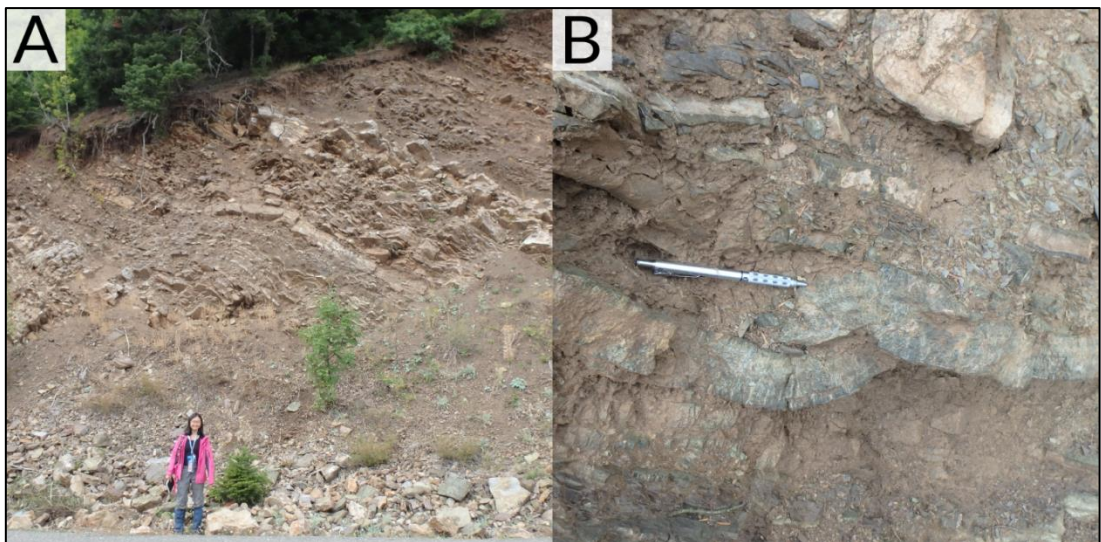


Fig. 3: Photographs illustrating features of the Pindos Flysch Group. A. Folds within flysch of ~5 m wavelength, best observed within the thicker beds of coarse sediment (-19340, -24885; 40.02670°N, 21.24192°E); B. Smaller scale folds of 10-50 cm wavelength within muddier beds are often accompanied by minor compressional faults within more competent beds of coarser material.

The Pindos Flysch found within the mapping area did not contain any fossils. The lack of fossils is suggestive of it having formed in a deeper marine environment than other sediments in the mapped area. The Cretaceous Duo Dendra flysch reported by Jones and Robertson (1991) does not seemingly appear to outcrop within the mapped area; if the Duo Dendra is present, then it is not easily distinguished from the Pindos Flysch group at field level.

2.1.2. Orliakas Group

The Orliakas Group is a sparry, fossiliferous limestone, and is the material forming the Orliakas scarp after which it is named (Fig. 4A). Fresh surfaces of the Orliakas limestone show an almost-crystalline white matrix; weathered surfaces are tinted a blue-grey, with draining routes down the mountain coloured a pale orange.

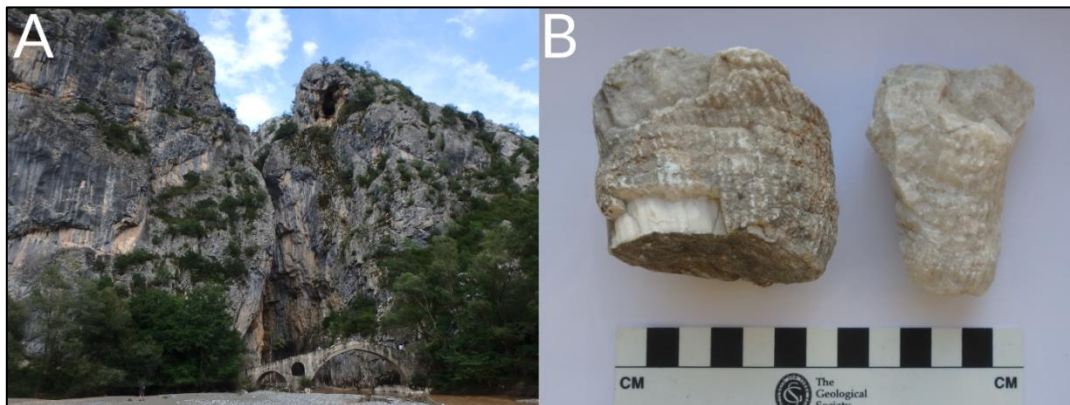


Fig. 4: Photographs illustrating features of the Orliakas Group limestone. A. Orliakas Group limestone forms the distinct ridgeline of Mount Orliakas, showing distinct blue-grey weathering. The photograph here is taken at Portitsa Gorge (-15365, -28250; 39.99579°N, 21.28804°E) B. Recrystallised rudist bivalves recovered from scree slopes around Orliakas.

Cretaceous rudist bivalves are commonly found in scree slopes around Orliakas or in outcrops of limestone (Fig. 4B). No internal structures are preserved within rudists, most likely as an effect of diagenetic recrystallisation; this may additionally explain why few primary sedimentary structures are preserved within outcrops of the limestone. Jones and Robertson (1991) place the Orliakas Group in the Cretaceous Santonian to Lower Campanian of the Late Cretaceous. Other fossils may be found in association with the rudist bivalves; however none were observed in the mapped area.

It is generally accepted that reefs were constructed upon topographic highs on the seafloor formed from the thrusting of ophiolitic material onto continental shelf (Rassios, 2011). This subsequently resulted in the development of the Orliakas Group as an unconformable, laterally discontinuous unit built upon ophiolitic basement. Outcrops within the mapped area are bound by faults, meaning that the lateral continuity of the Group is difficult to completely assess. A large area to the south of Mount Orliakas is covered by a clast-supported breccia of limestone pieces ranging from >1 cm to 20 cm in size, held by a micritic matrix. Whilst mostly structureless, the breccia is often distinctly bedded (e.g. at -17220, -27170; 40.00056°N, 21.26668°E) most commonly with a dip of no more than 30°. This breccia is commonly found along the major faults in the region bounding Mount Orliakas; this co-occurrence suggests that this breccia is Orliakas Group-related debris linked to seismicity coinciding with the uplift and structural development of Orliakas; the shallow dip angle of the breccia is likely the angle of repose of accumulating fault debris.

2.1.3. Mesohellenic Trough Sediment Group (MHS)

Mesohellenic Trough Sediment Group (MHS) can be subdivided into two formations in the mapped region, differentiated by period of deposition and subsequent geographical location (Zelilidis et al., 2002).

- The Kranea formation comprises a basal conglomerate overlain by deltaic and flood-plain sandstones and siltstones.
- The Eptahori Formation comprises conglomerate with interbedded sandstone and fan delta deposits, and overlies the Kranea Formation.

The Kranea Formation is found to the south of Orliakas; the Eptahori Formation to the north. The close resemblance of these two formations at outcrop level within the mapped area in addition to their clear geographical differentiation means that further differentiation is arbitrary; we therefore refer to the Group as a whole rather than to its subdivisions. Sediments of the MHS are generally heterolithic, often comprising alternating beds of medium-coarse sand and finer beds of muds or silt (Fig. 5A), comprised of poorly sorted yellow-tan angular clastic material. Some beds are rich in carbonate, present as invertebrate fossils or as a micritic mud. Calcitic veins are present within some joints in outcrops; these veins are secondary and unrelated to the initial deposition of the MHS.



Fig. 5: Photographs characterising the Mesohellenic Trough Sediment Group. A. Heterolithic beds exposed off a road at (-17675, -27160; 40.00583°N, 21.26139°E). The uppermost bed in the photograph hosts exceptional flute casts on its underside; B. The basal conglomerate of the Kranea Formation subdivision of the Group at (-16135, -27890; 39.99962°N, 21.27947°E). C. *Thalassinoides* trace fossils on a bedding surface at (-15480, -22850; 40.04034°N, 21.29001°E).

The base of the MHS is exposed to the south of Orliakas, and is a poorly sorted conglomerate of rounded, pebbly clasts ranging from 1 to 50 cm supported by a coarse sand matrix (Fig. 5B). Imbricated clasts within the conglomerate allow for measurement of bedding. The MHS overlies the other lithologies of the region unconformably. The abundance of faults, collapse structures, and overturning of beds makes the thickness of the MHS difficult to judge. Boudins are common within the sand beds to the south of Orliakas; these boudins weather in a distinct ‘onion-skin’ pattern comprising concentric layers. These observations support a nearshore marine depositional environment. Sedimentary sequences preserved in parts of the MHS show gradual coarsening up (e.g. -17960, -24770), suggesting some degree of deltaic input.

2.1.4. MHS palaeontology

Both trace and body fossils are commonly found within the MHS. Burrowing traces were found at localities in the MHS. Many *Thalassinoides* traces are found at (-15480,

-22850; 40.04034°N, 21.29001°E) (Fig. 5C), and *Chondrites* can be found as silty infills within muddy beds (e.g. at -17960, -24770; 40.02779°N, 21.25737°E).

The MHS bears many body fossils of shallow marine invertebrate metazoans, including bivalves, gastropods, brachiopods, foraminifera, corals, and bryozoans (Fig. 6). Ridged and smooth bivalve shell pieces up to 10 cm in length are very common in the MHS sandstones. Most shells appear to be recrystallised; primary shell material has been preserved in some localities. Death assemblages bearing many bivalve shell pieces were common within the coarse sandstones of the MHS; these beds are particularly well exposed on the road from Ziakas to Perivolaki.

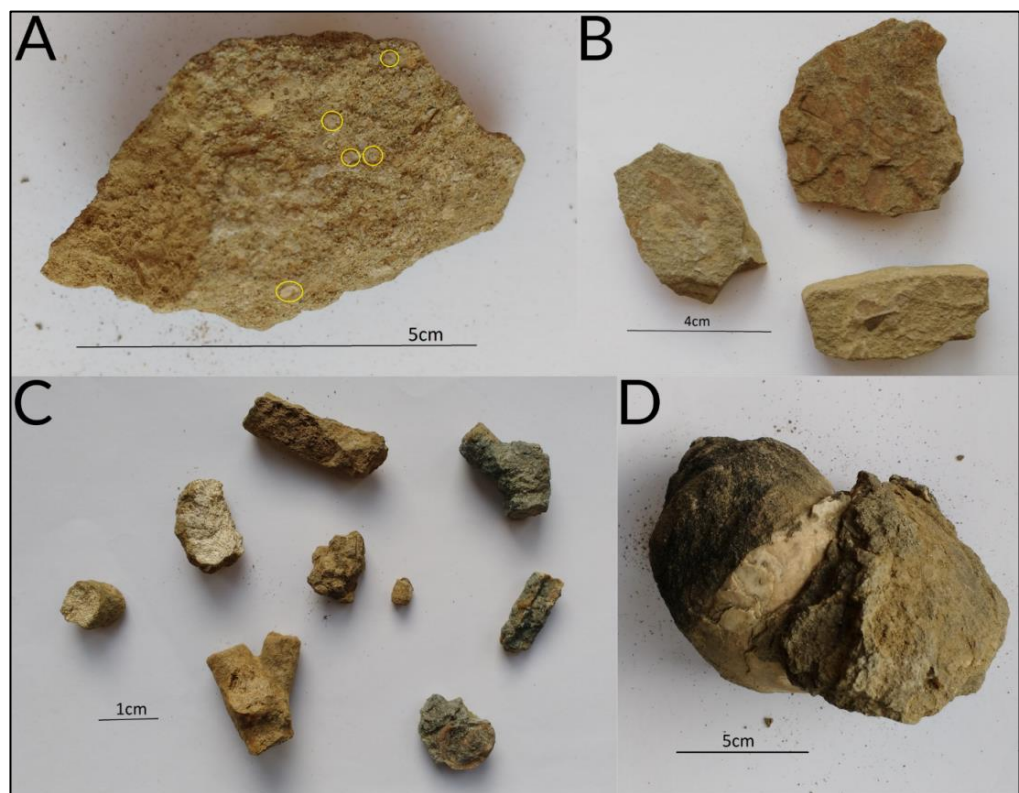


Fig. 6: A collection of photographs illustrating the variety of fossils present within the Mesohellenic Trough sediments. A. Foraminifera (highlighted by yellow circles); B. Angiosperm leaves oxidised to a red colour; C. Fragments of scleractinian corals; D. A large gastropod. Fossil localities are included in the text.

There are several localities within the MHS where fossilised leaves of angiosperm plants could be collected (e.g. -16220, -24840; 40.03022, 21.27924). Stems and veins of leaves are often still visible, and are coloured either a rusty red or black; they were most likely preserved as carbonaceous compressions, then pyritised. Those later exposed to air were oxidised to red colour.

Small phosphatised foraminifera can also be observed within the MHS; these foraminifera are a few millimetres in diameter with a flat, spiral-like shape. At (-15055, -26325; 40.01317°N, 21.29331°E) larger nummulitid foraminifera can also be observed within a death bed. Schleractinian coral was found at only one locality, and within a death bed (-16055, -24885; 40.02658°N, 21.28010°E). Varying levels of preservation were observed; only a few specimens have preserved internal structure in which polyps can be seen. Gastropods range in size from a few mm to 15 cm in length, and are mostly found to the north of Orliakas in the Eptahori Formation (e.g. -17400, -23810; 40.03707°N, 21.26414°E). Most small gastropods are turreted in shape whilst larger specimens are wider and turbinate. These gastropods are preserved with shell material intact.

This fossil evidence all suggests a dynamic nearshore environment of MHS deposition, which encouraged a thriving metazoan community, with sediment input and plant material from land.

2.2. AVDELLA MELANGE

The Avdella melange is a block-and-matrix melange (Raymond, 1984) that is mapped in the region as a single unit with immense lithological variability. The limited fossil preservation within melange blocks has given a Middle Triassic age for the oldest blocks (Ozsvrt et al., 2012). In the mapped area, the melange is best exposed east and west of the Pindos Flysch along the road running parallel to the northern face of Orliakas. The blocks of the Avdella melange are comprised of basaltic lavas, dolerites, gabbros, serpentinitised peridotites, limestones, and cherts, and range in size from centimetres to hundreds of metres. These blocks are set in a heterogeneous purple-red matrix comprising mudstone, sandstone, and shale. The matrix itself often comprises material from nearby melange blocks (e.g. evident serpentine in the matrix groundmass near serpentinite blocks). There is therefore difficulty when determining melange block from bedrock (e.g. peridotite/melange contact at (-20785, -26170; 40.01495°N, 21.22491°E). Contacts in these areas have been placed at the first appearance of the melange matrix, which is generally softer and easier to break from outcrop than expected from its constituent lithologies. The melange matrix is commonly found wrapping around small blocks (Fig. 7). While it is possible to determine imbrication of blocks (Ghikas et al., 2010), the blocks in the mapped area were only exposed along roads and paths, and hence limiting the measurement of block orientation in three dimensions.

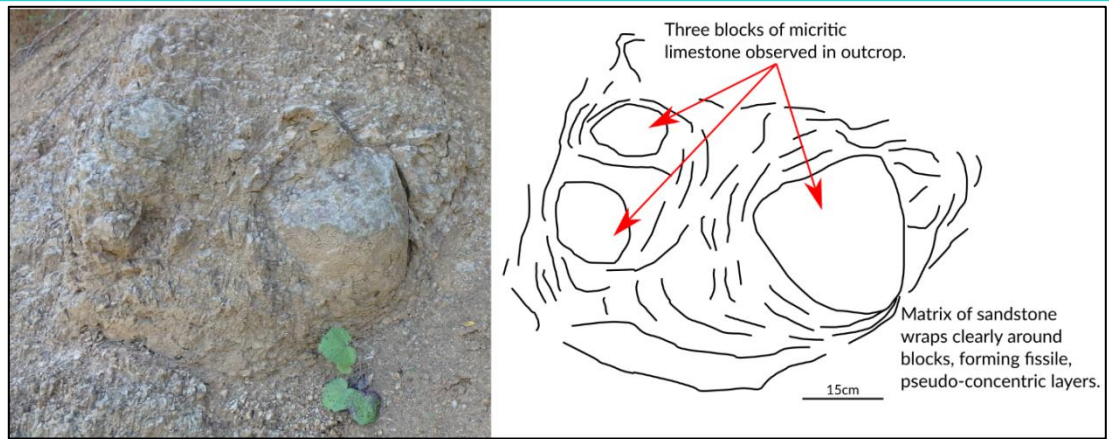


Fig. 7: Photograph and accompanying schematic diagram of limestone blocks within a fissile, wrapping melange matrix of unsorted sand-mud grade sand-mud-grade sediment (-18760, -24950; 40.02583°N, 21.25417°E).

The melange lacks fossils within its matrix, likely owing to its formation conditions. Its blocks however are from a variety of different lithologies, and some fossils are preserved within the larger limestone blocks (e.g. a preserved bivalve shell is exposed on the surface of a limestone block at -18005, -25015; 40.02533°N, 21.25759°E).

2.3. Pindos Ophiolite Group

The ophiolitic rocks in the mapped region are classified by Rassios and Moores (2006) as part of the underlying imbricates of the Dramala Complex within the overarching Pindos Ophiolite Group. To distinguish between the compositionally similar lithologies of the Pindos Ophiolite, we have used the BGS classification for igneous rocks, which differentiates mafic lithologies based on crystal size (Gillespie and Styles, 1999). The type section for these ophiolitic lithologies is along the road west of Spelio beginning at o (-18555, -26560; 40.01250°N, 21.25139°E) and ending at (-20450, -27405; 40.00389°N, 21.22972°E), which follows the ophiolite east-to-west from pillow basalt into serpentinised peridotite.

2.3.1. Ophiolitic basalts and dolerites

A series of fine grained lithologies occurs near the upper part of the ophiolite complex. As these lithologies tend to occur in rapid succession (often all within metres of each other) they have been grouped together as one unit with a noticeable degree of petrological variation. Each individual lithology within this mapped group is defined as follows.

Pillow basalts

The uppermost part of the ophiolite complex is dominated by pillow basalts around 1.5 m in diameter (Fig. 8). Their orientation can be determined from the shape of the outcrops and the positions of amygdales and vesicles on the outcrop surfaces. In the field, the rock is glassy, with occasional white and dark phenocrysts of 0.5 mm or less. Pillows are often found heavily brecciated, and coloured black/dark brown to red; the reddest pillows have noticeable chert exposed on pillow exteriors; the colour of the outcrop may be linked to the extent of silicification from chert the pillows have undergone. In thin section (Fig. 9A), the rock comprises phenocrysts (up to 1 mm) of plagioclase feldspar and clinopyroxene in a fine (<0.2 mm) groundmass of acicular plagioclase and altered volcanic glass. Extinction angle measurements of plagioclase feldspar crystals give a maximum of 37° , corresponding to An_{66} .

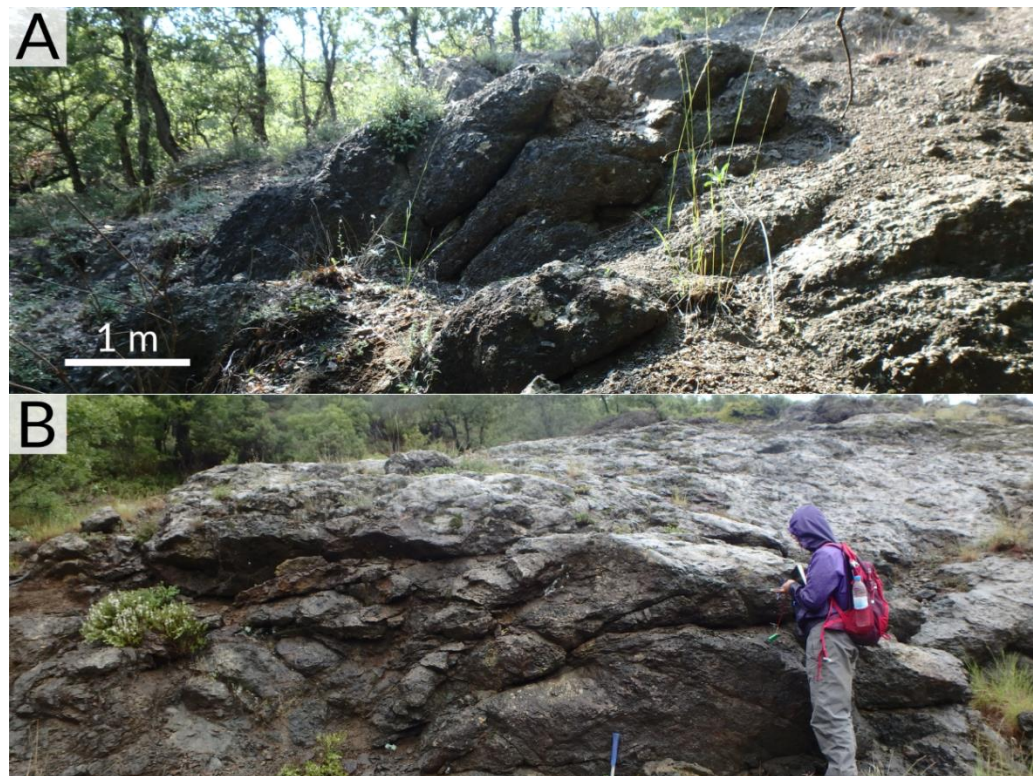


Fig. 8: Photographs of two pillow basalt localities within the mapped area. Localities are A.: (-17245, -27580; 40.00220°N, 21.26673°E), and B. (-17295, -28215; 39.99595°N, 21.26633°E).

Phenocrysts within the pillows suggest that the basalt has undergone transport from a crustal magma chamber in which crystals could accumulate and grow; the fine-grained nature of the rock and the presence of swallow-tail twins of plagioclase feldspar in the rock groundmass however are indicative of rapid cooling during

transport and eruption. Other than the hyaloclastic volcanic glass forming the groundmass, the rock is mostly unaltered relative to the successive lithologies in the ophiolite sequence; the fine-grained nature of the rock may prevent water from percolating through it.

Felsic dolerite

The lithology underlying the pillow basalt is a considerably coarser dolerite, which is seemingly more felsic due to its mesocratic colouration. No clear foliations or lineations are observed within it, but it is heavily jointed. The lithology is holocrystalline, with dark pyroxene and plagioclase crystals within a felsic matrix (all up to 1 mm in size). In thin section (Fig. 9B), the rock comprises plagioclase (50%), clinopyroxene (20%) and orthopyroxene (20%). Epidote is also present within the rock, however in trace quantities (<1%). The rock is granular, with all crystals generally no larger than a millimetre, and with little groundmass. Unusual textures are seen within the rock's constituent minerals. The clinopyroxene has been partially replaced by hornblende, which appears as higher birefringence blebs within the host pyroxene crystal. Hornblende has a distinct green-brown pleochroism, in contrast with the non-pleochroic clinopyroxene. Fine exsolution lamellae of pigeonite are also evident within clinopyroxene, indicative of a period of slow cooling. Plagioclase feldspar crystals additionally show chemical heterogeneities. Plagioclase crystal cores have an anorthite composition like the pillow basalts (An_{68} from extinction angles) with uniform extinction, but rims are primarily sodic plagioclase (An_{13}), and show undulose extinction. Both the formation of hornblende from pyroxenes and the presence of albite rims on the feldspars suggest that the rock has undergone some degree of low temperature hydrous metamorphism, likely soon after generation of the oceanic crust at the mid-ocean ridge. Low degrees of hydrous alteration probably affected the rims of the plagioclase whilst still hot, forcing their compositional change.

Bastite dolerite

The coarser grained material is followed by a heavily altered, cake-like lithology, which appears green in outcrop and breaks easily by hand (almost as a consolidated soil would). Plagioclase crystals of 0.2 mm and dark phenocrysts 2 mm in length can be identified within the crumbly groundmass of the rock. This extensive alteration of the rock is confirmed in thin section; the groundmass is dominated by plagioclase, and large phenocrysts are present of plagioclase (65%), clinopyroxene (20%), and bastite

serpentine (15%). Dark phenocrysts observed at hand specimen are serpentine crystals pseudomorphed to the shape of euhedral pyroxene (Fig. 9C). Groundmass plagioclase is sodic, with a composition of $\sim\text{An}_9$. This is difficult to confirm as many crystals now exhibit undulose extinction. In this rock, fluids have been able to permeate through, accelerating hydrous alteration.

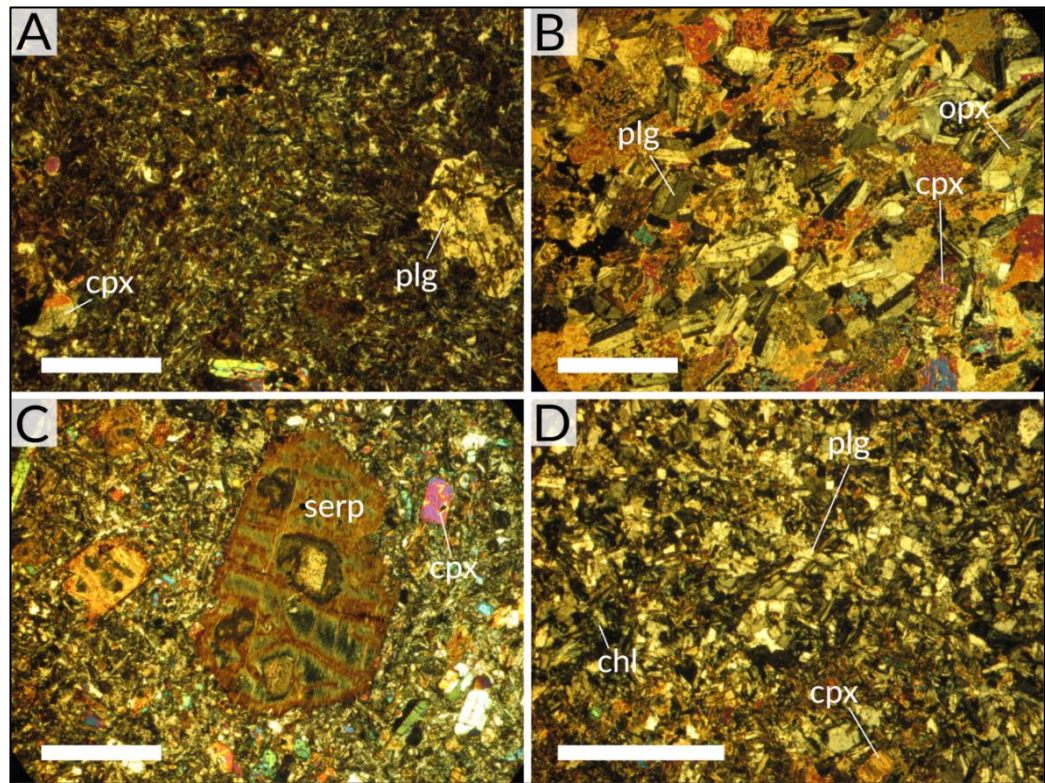


Fig. 9: Cross polarised photomicrographs of basalts and dolerites within the mapped area; nomenclature as found in the text. A. Fine-grained, glassy pillow basalt with phenocrysts of plagioclase feldspar and clinopyroxene, sampled at (-18555, -26560; 40.01250°N, 21.25139°E); B. Granular felsic dolerite comprising feldspars and partially amphibolitised pyroxenes, sampled at (-18570, -26445; 40.01248°N, 21.25111°E); C. bastite dolerite containing clinopyroxene-pseudomorphs of serpentine, sampled at (-18585, -26465; 40.00890°N, 21.25834°E); D. partially altered massive dolerite, sampled at (-18615, -26520; 40.01194°N, 21.25028°E). Scale bars (white bars) are 1 mm. *cpx* clinopyroxene, *plg* plagioclase, *opx* orthopyroxene, *serp* serpentine, and *chl* chlorite.

Massive dolerite

The altered material is succeeded by a series of dykes, which culminates in a massive, basaltic lithology coloured grey-blue in the field. This dolerite is known in the region

(also termed diabase by Rassios, 2011), and is generally fine grained, although occasional laths of plagioclase feldspar can often be seen up to 1 mm in length. Thin section shows a fine-grained (0.2 mm) texture of plagioclase and poorly defined clinopyroxenes; chlorite is also present within the groundmass (Fig. 9D). Plagioclase extinction angles give a composition of An_{67} , matching that of the lithologies stratigraphically above it. Hydrous alteration is evident within the rock; chlorite has grown in cavities and cracks within the rock, highlighting the openings through which water has permeated.

Discussion of upper-ophiolitic lithologies

The mineral components within the underlying dolerites are more altered than those within the basalt, on account of the basalt being finer grained. This textural difference may prevent the passage of water through the rock, limiting alteration, and instead partially hyaloclasticising the groundmass to form a brown altered product. The dolerites have been partially metamorphosed. Amphiboles occur sporadically both within and on the rims of the clinopyroxenes of the felsic dolerite. The presence of albite rims around more anorthositic plagioclase crystals in the same rock, as well as albites present within the bastite dolerite suggest that the metamorphic reaction was in amphibolite facies, after the actinolite-hornblende reaction but before garnet-forming reactions. Metamorphism must have only partially occurred for the preservation of igneous minerals and textures such as exsolution lamellae. A likely timing for this metamorphism would be intracrustal thrusting during ophiolitic obduction, when hotter crust could be in contact with the cooler, upper crust.

2.3.2. Ophiolitic cumulate gabbros

The region to the west of the exposed basalts and dolerites consists of hard, dense rock weathered an orange-grey colour. This lithology is difficult to break open; fresh surfaces reveal a coarse holocrystalline and granular matrix of dark olivine and white plagioclase feldspar, with occasional clinopyroxene (crystals 5 mm in diameter). Layering of clinopyroxene and olivine within the gabbros is observed in some outcrops (Fig. 10A), but is not consistent throughout the mapping area. In thin section (Fig. 10B), the rock shows a granular texture dominated by plagioclase feldspar. Olivine is also present as a significant constituent. Augite and orthopyroxenes form an oikocryst phase, which wraps around the other constituent minerals. From petrographic analysis, olivine is determined to be Fo_{86} , and plagioclase to be An_{66} . Plagioclase crystals remain mostly unzoned.

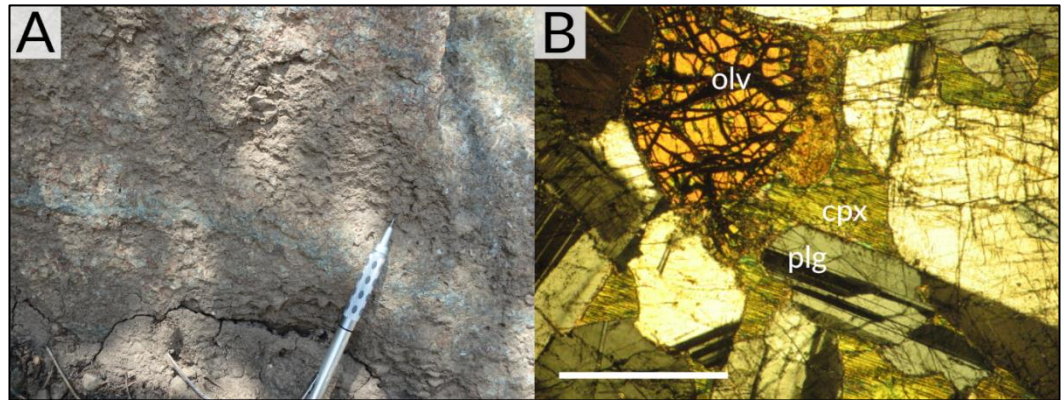


Fig. 10: Photographs of features within the gabbro of the Pindos Ophiolite. A. Field photograph of a planar band of clinopyroxene within ophiolitic gabbro at (-19935, -26800); B. Photomicrograph of gabbro under crossed polarised light, sampled at (-19110, -26395). Note the clinopyroxene oikocryst with exsolution lamellae. Scale bar of 1 mm. olv olivine, cpx clinopyroxene, and plg plagioclase.

The observed layering, pyroxene oikocrysts, the cooling lamellae within pyroxene, the large crystal sizes and the equilibrated grain boundaries suggest a cumulate origin for the gabbros. These rocks may have developed as magma reservoirs beneath mid-ocean ridges, hosting material that would eventually erupt as the pillow basalts and dolerites observed in the mapped area.

2.3.3. Ophiolitic peridotites

The peridotites outcropping in the mapping area has been serpentinised to form a brittle and very fine-grained rock, with a low specific gravity relative to the other igneous lithologies. Waxy serpentine is often found growing with no clear orientation along fractured planes and joints within the serpentinite. White serpentinites form within joints and cracks of outcrops. In some outcrops, foliations are marked through the serpentinite, marked by white and black zebra-like striping, or small mm-scale bands (Fig. 11A). These bands are also present in thin section; lizardite crystals no larger than 0.2 mm form along the flanks of opaque iron oxides generated from the serpentinisation reaction (Fig. 11B). The groundmass between the bands comprises tiny chrysotile crystals much smaller than 0.1 mm in size. The concentration of iron oxides along planes is most likely achieved through ductile shearing of hot peridotite either during oceanic crust formation or ophiolitic obduction.

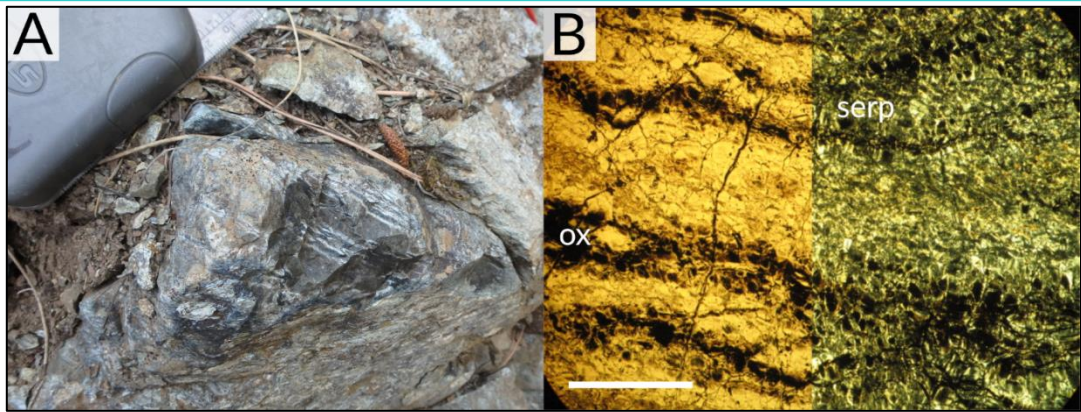


Fig. 11: Photographs illustrating observed banding within serpentinised ophiolitic peridotites. A. Field photograph of zebra-like striping of mm-scale at (-19975, -26895; 40.00890°N, 21.23444°E); B. Photomicrograph of banding under plane polarised and crossed polarised light, sampled at the same locality shown in Fig. 11A. Dark bands arise from layering of opaque oxides; light bands from serpentine. Scale bar of 1 mm. *ox* oxide, and *serp* serpentine.

The serpentinite is cut frequently by gabbroic and doleritic dykes. These dykes were likely injected when the surrounding material was still hot, as one dyke shows banding (-20535, -26790; 40.00929°N, 21.22792°E) – this banding is again likely to have resulted from shearing of the rock when ductile. This is evident in thin section as hydrous alteration has occurred along the cracks formed by the shears to form chlorite. As chlorite is a low temperature mineral, it must have formed after the ductile shearing took place, suggesting a phase of alteration after injection of the gabbroic material into the hot peridotite. Hydrothermal activity is noticeable within the serpentinite region of the ophiolite. Fine-grained, heavily serpentinised material forms vein-like features along the rock, and bronzite pegmatites also occur at (-20450, -27405; 40.00389°N, 21.22972°E).

2.4. Drift lithologies

The drift lithologies in the mapped region are alluvial deposits adjacent to the Venetikos river (e.g. near Portitsa Gorge), and glacial till deposited across the Pindos range. The till was deposited over the course of several Pleistocene glaciations in the Pindos, the last glaciation concluding 29,000 years ago at MIS 2 (Hughes et al., 2006). The alluvium is derived from the lithologies in the region and consists of cobbles up to 20 cm in size.

3. STRUCTURE AND DEFORMATION

To aid our structural description, we refer to the five panels illustrated in Fig. 12.

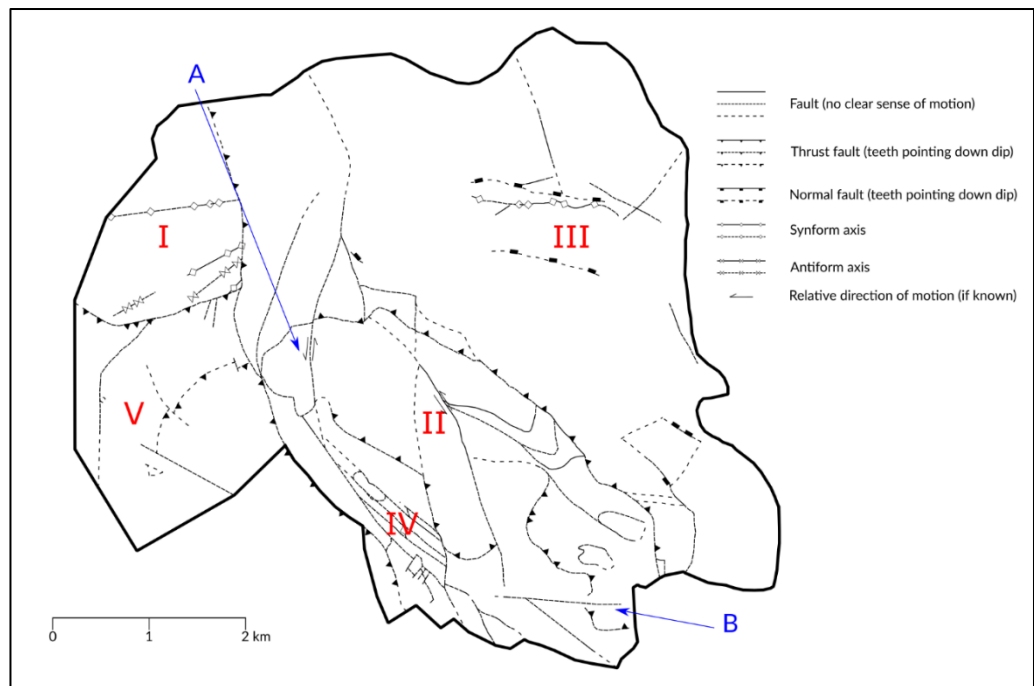


Fig. 12: Schematic map illustrating key structural geology in the mapped region. The map is split into five panels (I-V). Further distinction between panels are performed in the text.

3.1. Panel I. Flysch and melange

The flysch has been heavily folded throughout the mapped region (Figs 3 and 13). Folds can be tracked across the flysch by observing the course of its parallel beds. Fold axial planes trend NE-SW towards the ophiolite group, dipping both north and south, and become east-trending further north (Fig. 14). The folding is related to the direction of thrusting of the Pindos ophiolite during the initial emplacement phase; however, direction of folding from the position of hinge lines would be perpendicular to that expected for a NE-SW force for emplacement. A possible solution to this could be that locally, thrusting of the melange and the ophiolite occurred from the south-east rather than the south-west, leading to the NE-SW orientation of the axial planes seen. This would then ‘relax’ to a more E-W trend further north, as the folding would be affected by regional forces rather than local ones, resulting in components of local south-east force and regional south-west forces giving an overall north-south stress direction.

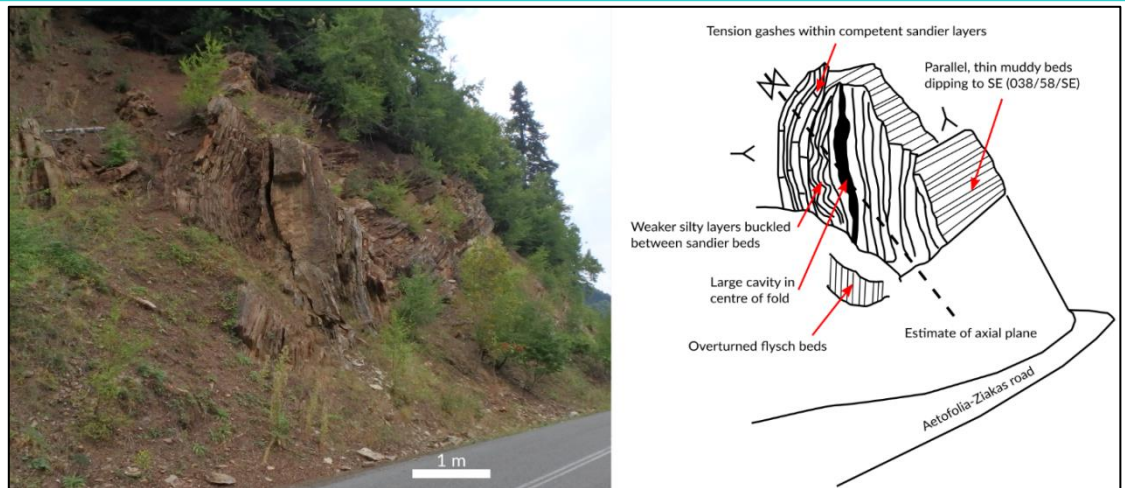


Fig. 13: Photograph and schematic sketch of a distinct antiform within the Pindos flysch at (-19545, -24715; 40.02803°N, 21.23959°E).

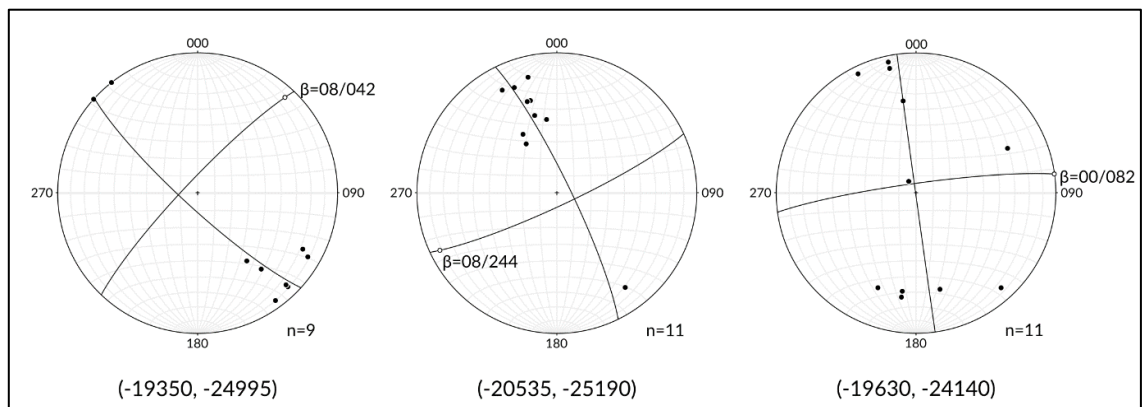


Fig. 14: Stereonets of folds within the flysch at three localities. The folds from left to right correspond with movement away from the melange-flysch contact in the direction of the north-west.

The flysch is discontinuous throughout the outcropping area. A synform on the western side seemingly coincides with an antiform on the eastern side of the flysch region (Fig. 13). This could be offset by a fault or further fold, although exposure by the road is good and would have revealed such a structure. One possibility could be a link between this fold and one observed along the road before the large antiform; however, the antiform is not present on the western part of the road. It is safe to conclude that the deformation undergone by the flysch is extremely complex, and requires further investigation to fully characterise. The flysch is bound on both sides by the Avdella melange. Near the flysch-melange contacts folding becomes much more intense, with wavelengths for folding of metre-scale at (-19330, -25010; 40.02500°N, 21.24222°E). As the faulted contacts appear to ignore any topography, they must be vertical at the surface, although cross sections by Rassios and Moores (2006) suggest that the fault is listric at depth.

The melange is in contact with the MHS to the east through a series of faults. Structure contours along parts of the melange-MHS contact suggests a shallow fault of 308/13/NE separating the two lithologies. The contact with the MHS at (-18240, -24495; 40.03013°N, 21.25469°E) appears steeply inclined; this contact is likely to be vertical as it cuts topography (Fig. 15A).

Structure within the melange is difficult to determine, due to the chaotic nature of the unit. The melange appears to develop a slaty cleavage around (-18200, -24880; 40.02655°N, 21.25505°E) (Fig. 15B). The stresses imposed on the fine-grained matrix appear to be aligned with the stress directions of nearby faults and are oriented north-south to match the steepness of the fault plane. Another example of chaotic structure within the melange are brecciated ridges at (-20355, -25445; 40.02140°N, 21.23039°E) (Fig. 15C). The strike of these ridges changes from 036 to 060 moving north and traces the strike of a nearby thrust fault separating melange from the ophiolite group.

3.2. Panel II. Mount Orliakas

The limestone of Mount Orliakas stands tall over the mapped region. This distinct topography implies that Orliakas limestone does not erode easily relative to the ophiolite and surrounding sediments. However, drainage paths down the mountain exploit planes of weakness in the limestone, permitting the identification of faults and localised zones of deformation.

The northern boundary of Orliakas is well defined topographically with steep, shear ridges along its length. The faulted contact between the limestone and the MHS has been suggested by many authors to be a dextral strike-slip fault (e.g. Zelilidis et al., 2002). However, no clear evidence was found in the field to support this.

The stratigraphic relationship between Orliakas and the surrounding lithologies in the north is best observed from Parorio (Fig. 16); Orliakas lies stratigraphically above pillow lavas near Portitsa Gorge, and a fault along the face of the mountain raises Orliakas above the Mesohellenic Trough.

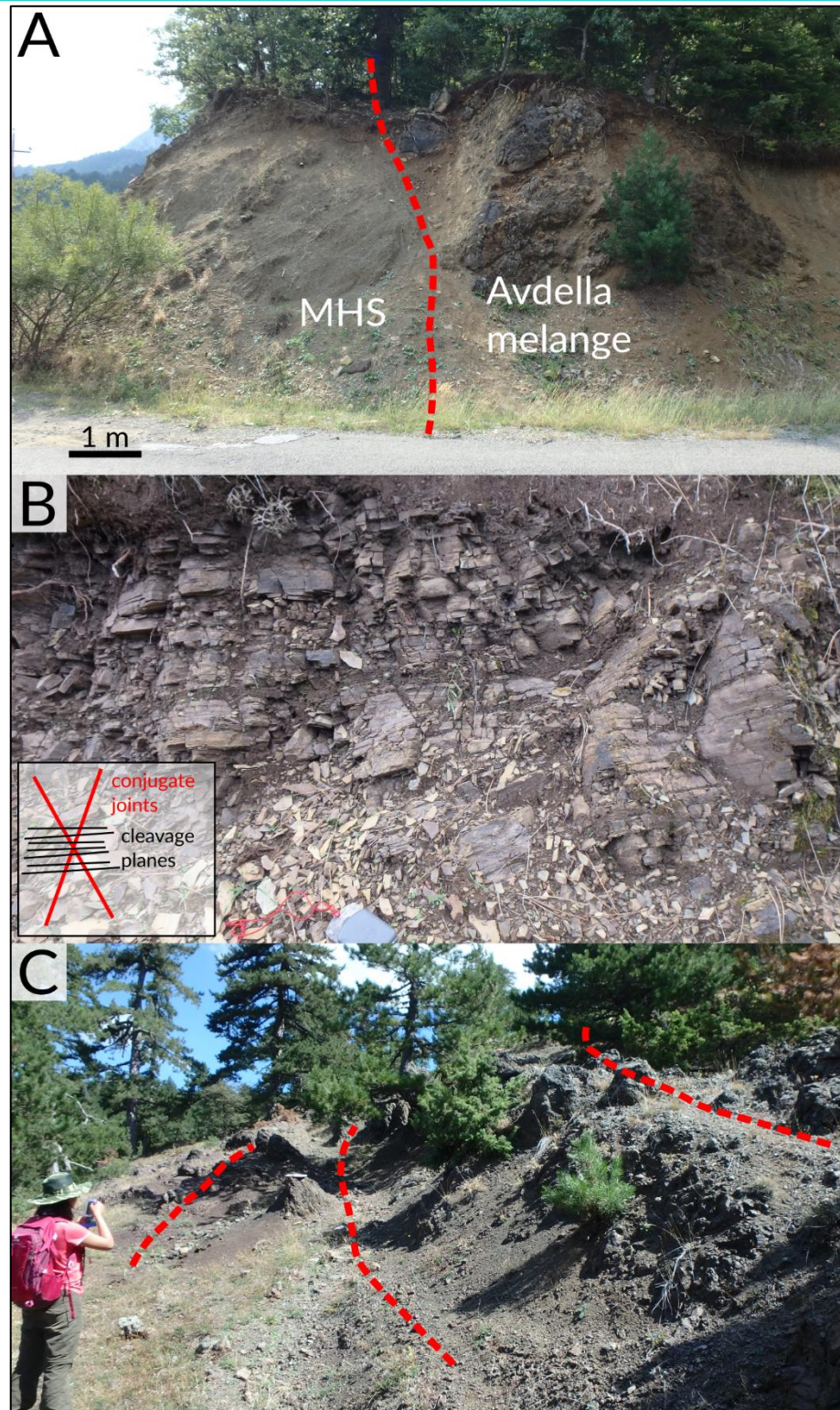


Fig. 15: Examples of erratic deformation structures within the melange. A. East-dipping beds of MHS lie in contact with a melange block at (-18240, -24495; 40.03013°N, 21.25469°E); B. Cleavages visible within the melange matrix at (-18200, -24880; 40.02655°N, 21.25505°E). Two clear joining directions are evident, suggesting a maximum principal stress normal to the observed cleavage planes; C. Ridges of melange at the ophiolite-melange contact at (-20355, -25445; 40.02140°N, 21.23039°E). Changes in the strike of the ridges are highlighted as red lines.

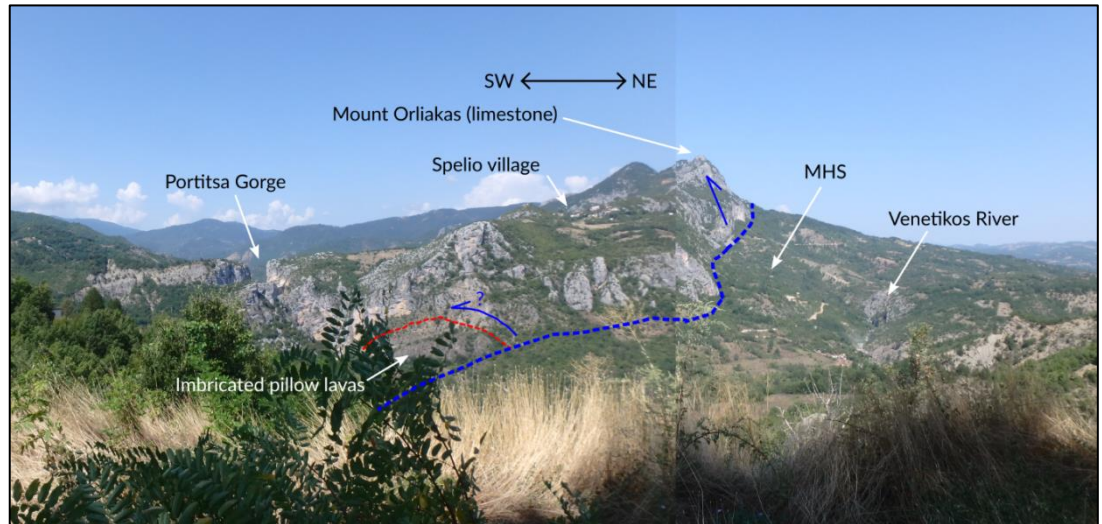


Fig. 16: Panoramic photographic of the viewpoint of Mount Orliakas and the western border of the Mesohellenic Trough from Parorio (-13935, -27950; 39.99718°N, 21.20638°E). The structural relationships between major lithological units are outlined, as are major geographical and geological features.

The southern boundary of Orliakas is poorly exposed owing to dense pine forest. Mapping within the forest gives a limestone-MHS contact roughly parallel to those of the faults further south within the MHS. A large fault at (-18575, -25575; 40.02054°N, 21.25085°E) (fault A in Fig. 12.) is evident in the westernmost part of Orliakas, where the mountain ridge is interrupted by a gully aligned near north-south. The strikes of deformed limestone ridges and the topographic offset suggest a sinistral movement; brittle shear patterns however suggest a dextral shearing motion oriented north-south. This dextral shear may be related to the original emplacement of Orliakas and linked to shallow angle thrust faults in the eastern part of Orliakas, with sinistral faulting occurring at a later stage.

Cemented layered breccias near faults within the limestone are observed along the borders of Orliakas dipping 18-38° away from the mountain (Fig. 17A); these are interpreted as cemented scree slopes. Other breccias are seen discontinuously within Orliakas itself; these breccias do not correlate on a large scale and are possibly related to minor faulting within Orliakas.

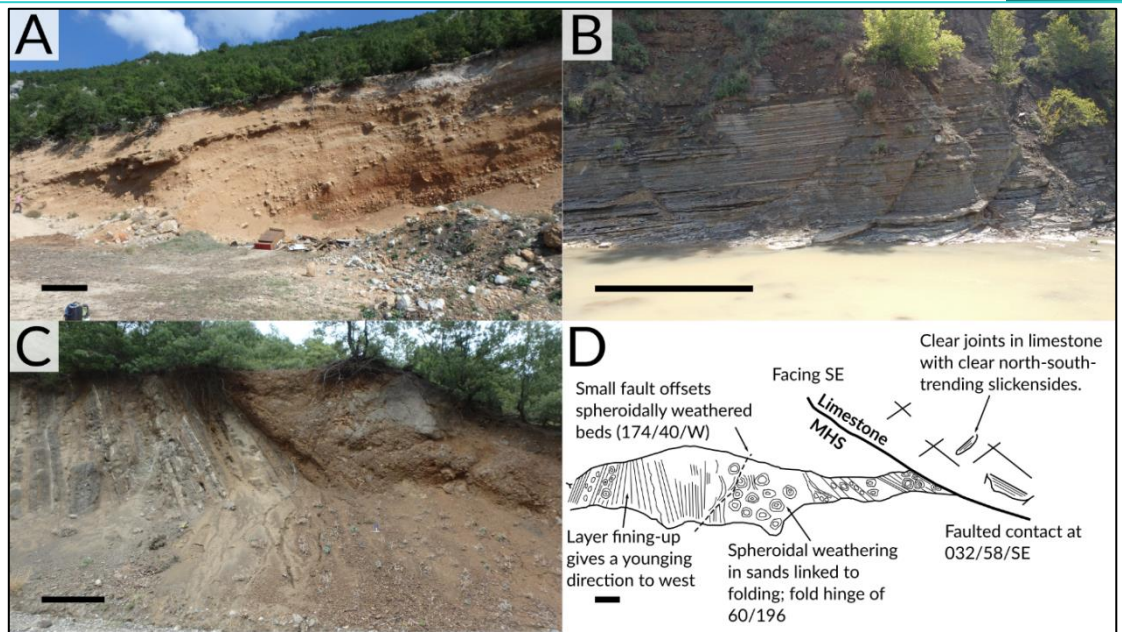


Fig. 17: Photographs and a schematic sketch of several structures observed within the mapped area. Scale bars of 1 m. A. Gently dipping limestone breccias at (-17125, -26835; 40.00944°N, 21.26639°E), interpreted as cemented scree slopes descending from Mount Orliakas; B. A series of small extensional faults cutting MHS at (-14770, -25050; 40.02498°N, 21.29511°E); C. A clear faulted contact between MHS and pillow basalts at (-17325, -27520; 40.00278°N, 21.26556°E). The two lithologies are separated by a fault breccia comprised primarily of basaltic clasts; D. Schematic sketch of the contact between MHS and Orliakas limestone at (-15620, -28235; 39.99664°N, 21.28562°E), the base of Portitsa Gorge. Scale bar of 1 m.

3.3. Panel III. North of Orliakas

The MHS strata to the north of Orliakas are upright, and dip east and southeast at $\sim 20^\circ$. Sedimentary beds are not heavily folded, and show only mild structural deformation. Deviation from shallow angle beds arise near normal faults within the basin or due to localised gravitational collapse. Most faults within the northern MHS are minor and are oriented north-south (Fig. 17B). Many of the smaller outcrop scale faults appear to be normal with displacements of a few metres at most. These faults are sediment collapse structures that partially accommodate extensional deformation during basin development. In the south-west part of the mapped area, there is an isolated area of Orliakas Limestone faulted on all sides. Some of these contacts can be seen in outcrops; the rest can be inferred from the geomorphology of the Venetikos river and local deformation.

3.4. Panel IV. South of Orliakas

South of Orliakas, the MHS is bound in the north by the Orliakas Group limestones, and to the south and west by the Pindos Ophiolite. The MHS itself is cut by a complex series of NW-SE trending oblique thrust faults, matching the trend of faults associated with the Mesohellenic fault system. In the field, they are determined by outcrops of brecciated material separating MHS beds with different dipping directions, or by sudden change in lithology forming ribbons of basement units outcropping in the area (Fig. 17C). These faults are vertical as they cut local topography. MHS beds strike NW-SE in this region, following the trend of these nearby faults. The dip of MHS varies to near-upright close to a fault, implying a close relationship between deformation and faulting. A noticeable fold within the MHS occurs at (-17600, -27465; 40.00323°N, 21.26244°E); one limb of this fold is oriented with a nearby fault.

Portitsa Gorge (-15365, -28250; 39.99579°N, 21.28804°E) lies at the most easternmost point of the mapping area and stands ~150 m above the Venetikos valley (Fig. 4A). The relationship between the limestone and the MHS to the south of Orliakas is best seen at this gorge, where the limestone directly overlies sediments, along a contact measured at 032/58/SE (Fig. 17D). For the Venetikos River to carve its way through the limestone rather than the arguably softer surrounding sediments there must be both a) a plane of weakness within the limestone and b) some degree of uplift to allow incision of the river into the limestone. We therefore suggest that there is a fault trending E-W concealed by the Venetikos river, along which the gorge could form, which also accounts for the difference in basal MHS either side of the river, which occurs without the clear presence of a large fold structure (fault B in Fig. 12.). Further evidence arises from shear structures within the gorge itself; slickensides on joints at (-15620, -28235; 39.99664°N, 21.28562°E) are oriented trending north-south, and orthogonal to the primary fault. Large faults present within the gorge arise from likely later deformation.

3.5. Panel V. Ophiolite

The mapped region of the Pindos Ophiolite primarily shows the upper crustal portion of oceanic lithosphere. Traversing east to west moves down the crustal section, from pillow basalts to dykes and dolerites, and then into cumulate gabbros and peridotites; this matches the Penrose model for oceanic crust (e.g. Dilek, 2003).

The lateral distance from pillow basalts to serpentinised peridotites is at its greatest ~2.5 km. In contrast, the thickness of typical oceanic crust is known to be 5-8 km (e.g. White et al. 1992), suggesting that some degree of telescoping and imbrication has occurred within the ophiolite, most likely during emplacement. No distinct sheeted dyke sections occur in the mapping area, and small regions of troctolite cumulate occur outside the main body of the unit (-20730, -26130; 40.01528°N, 21.22555°E), implying that the ophiolite in the mapping area has been dismembered. The telescoping is also likely to have been taken up by smaller shears and fractures throughout the entire ophiolite, rather than a few major faults. Brittle-phase ramp shears are common in the serpentinite region of the ophiolite (Fig. 18A). Fig. 18B shows an analysis of brittle shears within the ophiolite, clearly indicating bidirectional shear orientations – those dipping east and south-east, and those north-west and north. This would suggest that deformation within the ophiolite has occurred in a generally north-south direction, similar to the NE-SW direction suggested by Rassios and Moores (2006).

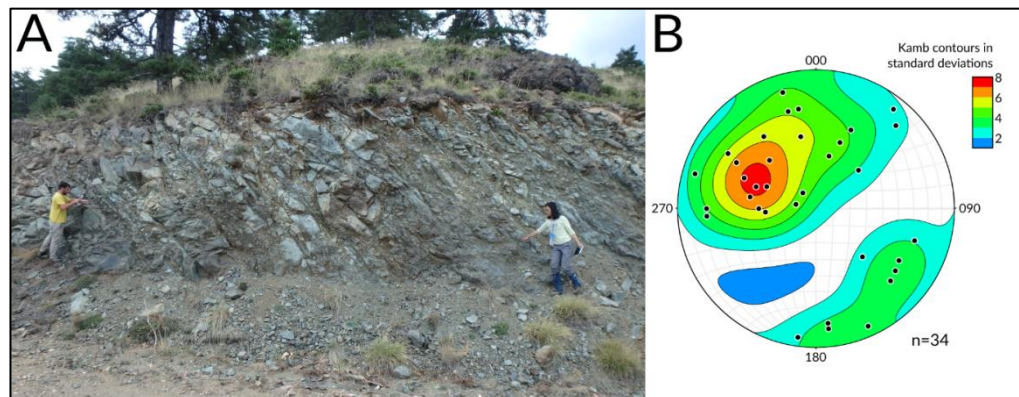


Fig. 18: A. Brittle-phase ramp shears within serpentinite at (-20350, -27475; 40.00306°N, 21.23028°E); the direction of motion suggested by these shears imply that the top of the structure moved from the left to the right of the page; B. Contoured plot of Reidel shears within the serpentinite. Poles to shear planes are concentrated to in the north and south of the stereoplot.

In the region adjacent to the Venetikos River, the ophiolite shows great petrological variation over a short distance; pillow basalt, dolerite and gabbro sequentially occur in rapid succession from north to south. Due to the difficulty of accessing this area, major faults are uncertain, but one solution is offered in our map of a series of NE-verging ophiolite 'chunks' offset by minor vertical faults. Faults are also difficult to follow along the forested western ridges of Orliakas. As such the boundary between serpentinised peridotites and the gabbros is very uncertain. A possible solution to the outcrop patterns is suggested on our map, taking the contact between the two

lithologies to be a fault striking north-east, so the southern part of the ophiolite is offset from the rest of the serpentinite. Although mineral lineations and foliations can be seen within the ophiolitic rocks, they do not correlate over the field area. They have likely been displaced and rotated due to imbrication of the ophiolite, and hence are discontinuous.

4. COUNT OF COBBLES IN THE KRANEA FORMATION

Statistical analyses of cobbles (similar to that performed by the *Aliakmon Legacy Project*, Rassios et al., 2016) were performed at two localities in the area, albeit at a smaller scale (100 cobbles per locality in contrast to the 10,000 at Aliakmon). The first was done within the Venetikos River at (-15680, -28230; 39.99620°N, 21.28514°E), and another within the basal conglomerate of the MHS (-16135, -27890; 39.99958°N, 21.27951°E), with the objective of comparing the lithologies, sizes, and shapes of the cobbles between the two settings. Using this analysis, the basal conglomerate of the Kranea Formation can be directly compared to a modern cobble deposit supplied solely from the Pindos Mountains. The basal MHS and the cobbles within the Venetikos yield different proportions of material (Fig. 19). The Venetikos bears more igneous lithologies, derived from the Pindos ophiolite to the west. The MHS bears more Orliakas Group and non-Orliakas limestones than the river (non-Orliakas limestone is defined as non-sparry limestone that cannot be readily be identified as Orliakas Group.).

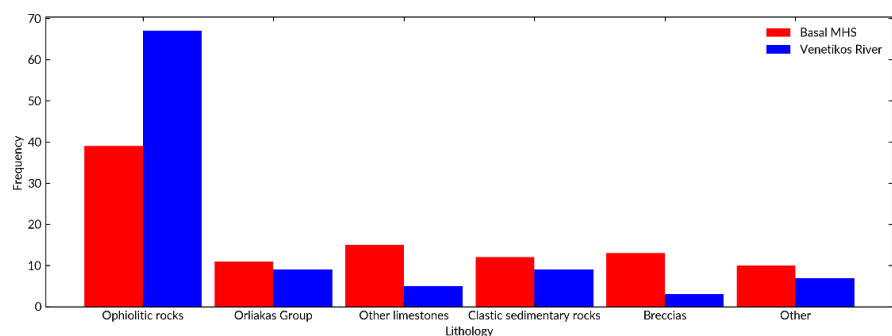


Fig. 19: Categorized count of different lithologies comprising 100 cobbles each from the basal conglomerate of the MHS and from the Venetikos River.

There are some lithologies not found within the mapping region. Banded amphibolite is found in both the MHS and the Venetikos, derived from the metamorphosed sole of the ophiolite that does not outcrop within the mapped area. Likewise, other lithologies not local to the mapping area are found within the MHS. These lithologies may only have been derived from the Pelagonian margin, and must therefore have been derived from the east as

opposed to the west. The mean size of cobbles found in the MHS is greater than those within the Venetikos, and large outliers are common in the MHS (Fig. 20A) in contrast to the river. The deposition of larger material requires higher energy, which is not reflected in the river sediments. This is also suggested by the cumulative frequency graphs for the two localities (Fig. 20B). The shapes of the frequency curves are initially similar, showing a steep gradient from 0 to 8 cm. There is a decline in the gradient from this point for the MHS curve, illustrating the influence of larger cobbles in the distribution. The setting for basal MHS deposition was therefore similar to the modern Venetikos, with occasional higher energy events depositing significantly larger material. MHS cobbles are smoother and more spherical than those of the Venetikos (Figs 20C and 20D). The rate of sediment supply to the Venetikos is therefore faster than the rate of cobble smoothing. The smoother cobbles of the MHS suggest either low transport speeds allowing a greater degree of smoothing or long transport distances. This evidence suggests that both the Pelagonian margin and the Pindos Ophiolite have provided clastic input into the Mesohellenic sediments. This could be confirmed further by extensive palaeoflow analyses within the MHS; whilst some data was collected on palaeoflow (e.g. ripple casts can be measured at -17675, -27160), the data collected across the mapped area was sparse and did not correlate.

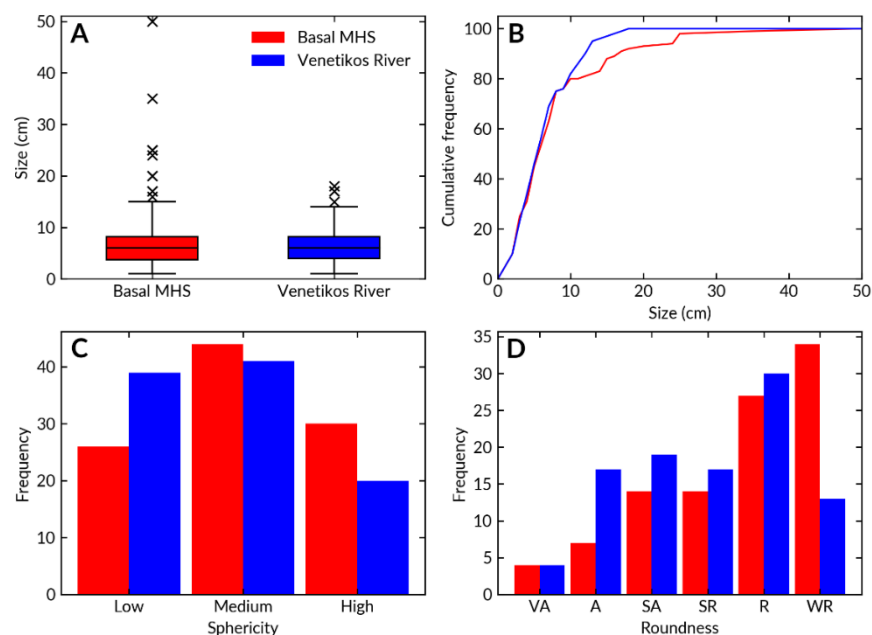


Fig. 20: Statistical analysis of 100 cobbles each from the basalt conglomerate of the MHS and the Venetikos River. A. Box plots comparing size distributions; B. Cumulative frequency plots illustrating differences in cobble size distribution; C. Plot illustrating differences in cobble sphericity; D. Plot illustrating variations in cobble roundness.

5. SUGGESTED GEOLOGICAL HISTORY

A geological history for the region is given below, and pictorially summarised (Fig. 21).

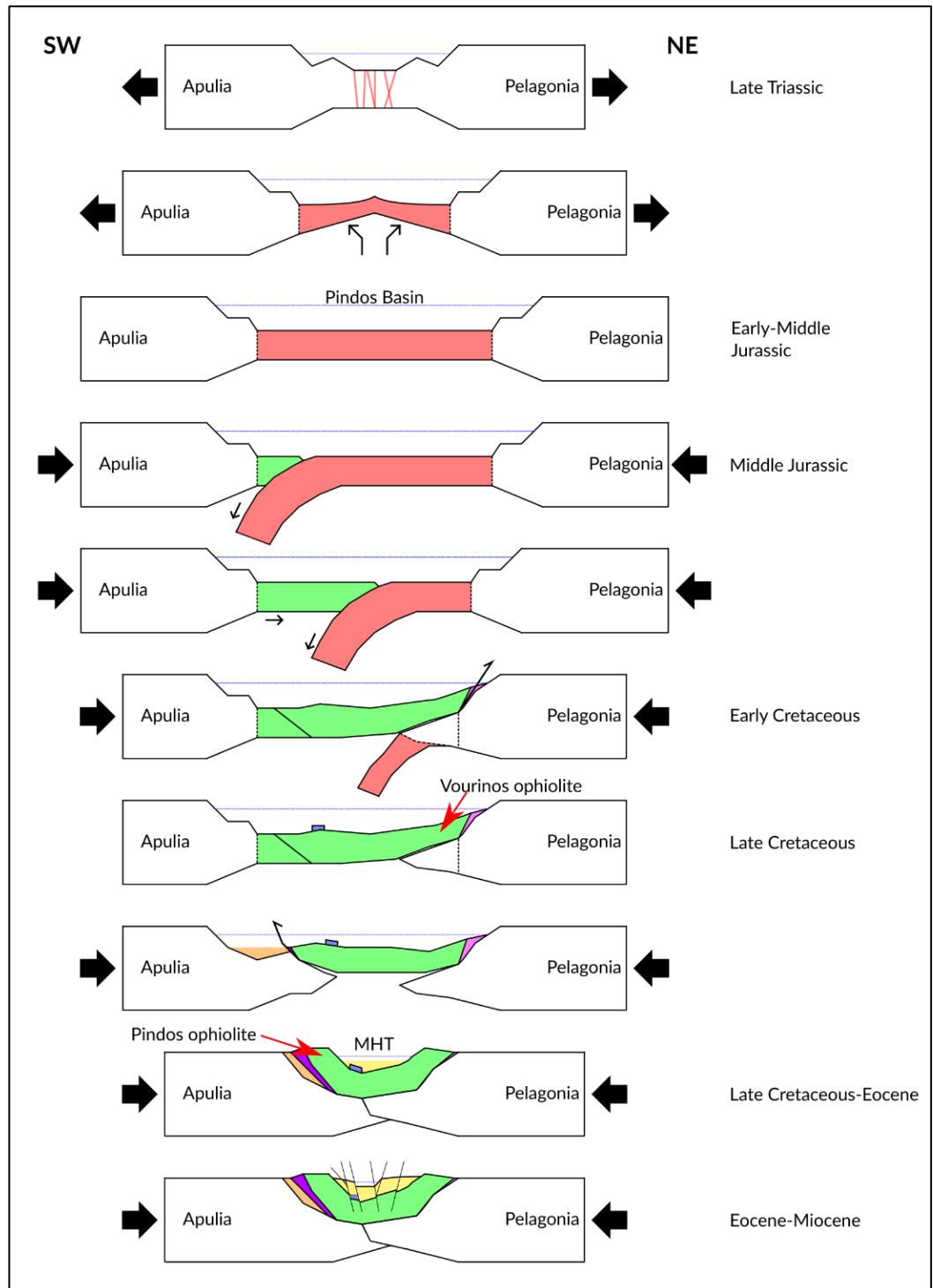


Fig. 21: Suggested geological history for the formation and development of the Greveniotiki Pindos Mountains, redrawn after Ghikas et al. (2010).

5.1. Earliest history

The oldest rocks recorded in the Pindos are blocks within the Avdella melange. These blocks are representative of the lithological formations making up the upper crust along the obduction direction of the ophiolite. As mid-ocean ridge basalts are preserved within the Avdella melange, early rifting within the Pindos Basin can be constrained to the Triassic Anisian, with radiolarian chert formation suggesting that deposition was likely beneath the CCD (Ozsvart et al., 2012).

5.2. Convergence

The presence of early shear structures within the Pindos Ophiolite are suggestive of the end of the extensional rifting regime and the beginning of a convergent regime leading to the emplacement of the Mesohellenic Ophiolite. The development of a western Pindos Basin subduction zone near the spreading ridge has been suggested by authors (e.g. Saccani et al., 2004). The emplacement of the Mesohellenic Ophiolite on the Pelagonian margin would have resulted in generation of an accompanying metamorphic sole and accretionary melange; these are recorded in association with the Vourinos Ophiolite. Subduction of the Pindos Basin had concluded by the Early Cretaceous. Passive development of the Pindos Basin continued with the growth of rudist reefs on the ophiolite.

5.3. Eocene obduction

Tectonic compression renewed during the Early Palaeogene. The Pindos Basin now developed as a subsiding foreland basin, within which the Pindos flysch accumulated (Faupl et al., 2007). The closure of the Pindos basin would have thrust the western half of the Mesohellenic Ophiolite over the flysch from the south to generate the complex imbrication and folding seen within the mapped area. Accretion of ground-up ophiolitic material and basin sediments would have formed the sub-ophiolitic Avdella melange (Ghikas et al., 2010).

5.4. Development of the Mesohellenic Trough

The formation of the Mesohellenic Trough began soon after final ophiolitic emplacement as a piggyback basin above the Pindos suture zone (Vamvaka et al., 2006). Initial sediment would have been deposited in a precursor basin, with sediment supply from both east (Pelagonian margin) and west (Pindos Ophiolite) to account for the variety in lithologies present in the MHS. Zelilidis et al. (2002) argue that the Kranea Basin to the south of Orliakas is a precursor basin to the Mesohellenic Trough, as seismic reflection sections show

sediment progradation from the north-east; our cobble analysis supports this point of view. Deposition of sediments was synchronous with basin formation.

The MHS in the mapping area has been affected by several of the phases of deformation categorised by Vamvaka et al. (2006). The earliest compressional regime recorded by these authors was oriented NE-SW; in our mapped area this is recorded by the thrust faults and exposed basement rocks to the south of Orliakas. The subsequent strike-slip faulting is evident within Mount Orliakas and the MHS to the north of Orliakas. A final stage of extensional deformation generates the normal faults seen within the Mesohellenic Trough. As many of the faults appear to be small-scale and collapse-related, it seems plausible that extension is continuing to this day in a north-south direction.

Quaternary glaciations resulted in the carving of U-shaped valleys, deposition of till throughout the region, and formation of geomorphological phenomena such as Portitsa Gorge (Hughes et al., 2007). Uplift is still ongoing to this day; this is evident from the steep, incised river valleys seen around the Venetikos.

6. ACKNOWLEDGEMENTS

This study arose from the mapping projects completed by the six authors during the summer of 2015, and was funded by the Department of Earth Sciences of the University of Cambridge, the Worts Travelling Scholars' Fund, the Gilchrist Expedition Fund, and Corpus Christi, Murray Edwards, St. John's, Robinson, Queens' and Gonville and Caius Colleges of the University of Cambridge. We thank Alex Copley, Dina Ghikas, and Anna Batsi and Anne Rassios for assistance during fieldwork and the production of this map and manuscript.

This work is dedicated to Alan Smith, who encouraged our work in the area, and supported this research from conception.

7. REFERENCES

Ananiadis, G., Vakalas, I., Zelilidis, A., and Tsikouras, B., 2004. Provenance of Pindos flysch deposits in Metsovo and Fournia areas using scanning electron microscopy and microanalysis. *Bulletin of the Geological Society of Greece*, 36, 534-541.

Brunn, J. H., 1956. Contribution à l'étude géologique du Pinde septentrional et d'une partie de la Macédoine occidentale. *Annales Géologiques du Pays Helleniques*, 7, 1-358.

- Dilek, Y., 2003. Ophiolite concept and its evolution. *Geological Society of America Special Papers*, 373, 1-16.
- Dilek, Y., and Furnes, H., 2009. Structure and geochemistry of Tethyan ophiolites and their petrogenesis in subduction rollback systems. *Lithos*, 113, 1–20.
- Dilek, Y., Furnes, H., and Shallo, M., 2007. Suprasubduction zone ophiolite formation along the periphery of Mesozoic Gondwana. *Gondwana Research*, 11, 453–475.
- Faupl, P., Pavlopoulos, A., and Migiros, G., 2007. Provenance of Flysch Sediments and the Palaeogene-Early Miocene Geodynamic Evolution of the Hellenides: A Contribution from Heavy Mineral Investigations. *Developments in Sedimentology*, 58, 765–788.
- Ghikas, C., Dilek, Y., and Rassios, A. E., 2010. Structure and tectonics of subophiolitic mélanges in the western Hellenides (Greece): Implications for ophiolite emplacement tectonics. *International Geology Review*, 52, 423–453.
- Gillespie, M., and Styles, M., 1999. BGS rock classification scheme, Volume 1. *Classification of igneous rocks*. British Geological Survey, Research Report. Ref no, RR/97/002.
- Hughes, P. D., Gibbard, P. L., and Woodward, J. C., 2007. Geological controls on Pleistocene glaciation and cirque form in Greece. *Geomorphology*, 88, 242–253.
- Hughes, P. D., Woodward, J. C., Gibbard, P. L., Macklin, M. G., Gilmour, M. A., and Smith, G. R., 2006. The Glacial History of the Pindus Mountains, Greece. *The Journal of Geology*, 114, 413–434.
- Jones, G., and Robertson, A. H. F., 1991. Tectono-stratigraphy and evolution of the Mesozoic Pindos ophiolite and related units, northwestern Greece. *Journal of the Geological Society*, 148, 267–288.
- Liati, A., Gebauer, D., and Fanning, C. M., 2004. The age of ophiolitic rocks of the Hellenides (Vourinos, Pindos, Crete): First U–Pb ion microprobe (SHRIMP) zircon ages. *Chemical Geology*, 207, 171–188.

Memou, G., and Skianis, G., 1991. Interpretation of aeromagnetic data in the Pindos–Vourinos region—part one: Qualitative analysis. Internal Report, Institute of Geology and Mineral Exploration, Athens.

Ozsvárt, P., Dosztály, L., Migiros, G., Tselepidis, V., and Kovács, S., 2012. New radiolarian biostratigraphic age constraints on Middle Triassic basalts and radiolarites from the Inner Hellenides (Northern Pindos and Othris Mountains, Northern Greece) and their implications for the geodynamic evolution of the early Mesozoic Neotethys. *International Journal of Earth Sciences*, 101, 1487–1501.

Papanikolaou, D., 2009. Timing of tectonic emplacement of the ophiolites and terrane paleogeography in the Hellenides. *Lithos*, 108, 262–280.

Rassios, A. E., 2011. A geologist's guide to the Greveniotiki Pindos, Greece. Athens: Institute of Geology and Mineral Exploration.

Rassios, A., Grieco, G., Batsi, A., Myhill, R., and Ghikas, D., 2016. Preserving the non-preservable geoheritage of the Aliakmon river: A case study in geo-education leading to cutting-edge science. *Bulletin of the Geological Society of Greece*, 50, 255–264.

Rassios, A. E., and Moores, E. M., 2006. Heterogeneous mantle complex, crustal processes, and obduction kinematics in a unified Pindos-Vourinos ophiolitic slab (northern Greece). *Geological Society, London, Special Publications*, 260, 237–266.

Rassios, A. E., and Dilek, Y., 2009. Rotational deformation in the Jurassic Mesohellenic Ophiolites, Greece, and its tectonic significance. *Lithos*, 108, 207–223.

Rassios, A. E., and Smith, A. G., 2000. Constraints on the formation and emplacement age of western Greek ophiolites (Vourinos, Pindos, and Othris) inferred from deformation structures in peridotites. *Geological Society of America Special Papers*, 349, 473–484.

Raymond, L. A., 1984. Classification of melanges. *Geological Society of America Special Papers*, 198, 7–20.

Saccani, E., and Photiades, A., 2004. Mid-ocean ridge and supra-subduction affinities in the Pindos ophiolites (Greece): Implications for magma genesis in a forearc setting. *Lithos*, 73, 229–253.

Smith, A. G., and Rassios, A., 2003. The evolution of ideas for the origin and emplacement of the western Hellenic ophiolites. *Geological Society of America Special Papers*, 373, 337–350.

Smith, A. G., 1993. Tectonic significance of the Hellenic-Dinaric ophiolites. *Geological Society, London, Special Publications*, 76, 213–243.

Thuizat, R., Whitechurch, H., Montigny, R., and Juteau, T., 1981. K-Ar dating of some infra-ophiolitic metamorphic soles from the Eastern Mediterranean: New evidence for oceanic thrustings before obduction. *Earth and Planetary Science Letters*, 52, 302–310.

Vamvaka, A., Kiliass, A., Mountrakis, D., and Papaoikonomou, J., 2006. Geometry and structural evolution of the Mesohellenic Trough (Greece): A new approach. *Geological Society, London, Special Publications*, 260, 521–538.

White, R. S., McKenzie, D., and O’Nions, R. K., 1992. Oceanic crustal thickness from seismic measurements and rare earth element inversions. *Journal of Geophysical Research*, 97 (B13), 19683-19715.

Zelilidis, A., Piper, D. J. W., and Kontopoulos, N., 2002. Sedimentation and basin evolution of the Oligocene-Miocene Mesohellenic basin, Greece. *AAPG Bulletin*, 86, 161–182.